

# New Insight Into The Spatial Autoregressive Model of Industrial Wastewater Discharge In The Yellow River Basin

Libo Xia (✉ [201514321@stu.ncwu.edu.cn](mailto:201514321@stu.ncwu.edu.cn))

North China University of Water Resources and Electric Power <https://orcid.org/0000-0002-4646-9547>

Zhiliang Wang

North China University of Water Resources and Electric Power

Shuang Du

North China University of Water Resources and Electric Power

Decun Tian

North China University of Water Resources and Electric Power

Feng Chen

North China University of Water Resources and Electric Power

---

## Research Article

**Keywords:** Yellow River Basin, Industrial Wastewater Discharge, Spatial Autoregressive, Environmental Kuznets Curve, Moran Index, Bayesian

**Posted Date:** December 16th, 2021

**DOI:** <https://doi.org/10.21203/rs.3.rs-1122988/v1>

**License:**  This work is licensed under a Creative Commons Attribution 4.0 International License.

[Read Full License](#)

---

1      **New Insight into the Spatial Autoregressive Model of Industrial**  
2      **Wastewater Discharge in the Yellow River Basin**

3

4            Libo Xia<sup>a,\*</sup>, Zhiliang Wang<sup>b</sup> , Shuang Du<sup>a</sup>, Decun Tian<sup>b</sup>, Feng Chen<sup>a</sup>

5

6        <sup>a</sup> *School of Environmental and Municipal Engineering, North China University of*  
7        *Water Resources and Electric Power, Zhengzhou, 450045, China*

8        <sup>b</sup> *College of Water Resources, North China University of Water Resources and*  
9        *Electric Power, Zhengzhou, 450045, China*

10

11      \* Corresponding author, Libo Xia. E-mail address: 201514321@stu.ncwu.edu.cn  
12

13      **Abstract**

14      This article has carried out a statistical analysis of the industrial wastewater  
15      discharge (IWD) and gross regional product (GRP) of 79 cities in the Yellow River  
16      Basin from 2003 to 2019. By calculating the Moran index of IWD and GRP, the study  
17      has found that a certain spatial autoregressive in space. There is an environmental  
18      Kuznets curve (EKC) between the environmental pollution and economic  
19      development of cities in the Yellow River Basin, and a spatial autoregressive is  
20      modelled by a set of random effects that are assigned a conditional autoregressive  
21      prior distribution. In the Bayesian environment, Markov chain Monte Carlo (MCMC)  
22      is used for inferencing, and the spatial weight matrix is selected to be U-shaped  
23      matrix, and the error of the model is minimized. The parameter posterior distribution  
24      results of the model showed that the GRP did not show a significant decline. The  
25      modified EKC showed that the discharge of industrial wastewater in the entire Yellow  
26      River Basin will be reduced. Generally, cities with high pollutant emissions should  
27      learn from other cities to reduce emissions, and cities with low GRP need to increase  
28      local economic development.

29      **Keywords:** Yellow River Basin; Industrial Wastewater Discharge; Spatial  
30      Autoregressive; Environmental Kuznets Curve; Moran Index; Bayesian

31

32     **1 Introduction**

33       As the mother river of China, the Yellow River's ecological environment is of far-  
34       reaching significance to the great rejuvenation of the Chinese nation. Through the  
35       analysis of the IWD of each city in the Yellow River Basin, suggestions are provided  
36       for the next step in the environmental pollution control of the Yellow River Basin. The  
37       problems of environmental pollution and economic development have been studied in  
38       the 1990s, and it was found that economic growth brought an initial stage of  
39       deterioration, followed by an improvement stage (Grossman and Krueger  
40       1995)(Selden and Song 1994). However, from the clean agricultural economy to the  
41       polluting industrial economy, some people questioned the existing evidence. The  
42       pollution caused by the environment is reduced, and the corresponding economic  
43       income level has not been agreed, and may lead to the demise of the classic EKC  
44       (Dinda 2004) (Stern 2004), the evidence for the existence of EKC was also questioned  
45       (Kijima et al. 2010). After a certain period of research on environmental pollution and  
46       economic development, it was found that environmental pollution was not only  
47       related to economic levels, but many other factors were slowly being taken into  
48       account (Managi 2006). Research on economic development and air pollution was  
49       closely related, the regional differences in the relationship between haze pollution and  
50       economic growth (Du et al. 2018). A survey of the empirical literature on carbon  
51       dioxide emissions found that EKC's estimation of carbon dioxide emissions was  
52       essentially uncertain (Shahbaz and Sinha 2019). China's environmental pollution had  
53       obvious spatial autoregressive, and economic development and environmental  
54       pollution present an inverted U-shaped curve (Cheng et al. 2017). Based on the

55 Bayesian model averaging method, the influencing factors of air pollution was  
56 analyzed, which proved the existence of EKC (Lin and Zhu 2018). Economic  
57 globalization will increase the degree of environmental pollution and had an impact  
58 on the ecological footprint, and the inverted U-shape was existed (Ulucak and Bilgili  
59 2018). The treatment of environmental pollution should implement different measures  
60 according to different spaces and different stages of development (Zhao et al. 2019).  
61 And industrial transfer and energy consumption structure were determinants of  
62 pollutant emissions in China (Li et al. 2020). In order to accelerate EKC to reach the  
63 turning point faster, it was necessary to promote renewable energy consumption (Yao  
64 et al. 2019). And emissions and income inequality had a major impact on the EKC  
65 turning point (Ridzuan 2019).

66 When calculating the relationship between environmental pollution and economic  
67 development, not just the total statistics and the environmental pollution and  
68 economic development of each city, but also the relationship between the spatial  
69 location and the calculation of its temporal and spatial characteristics. The  
70 Geographically Weighted Regression (GWR) model greatly improves the  
71 performance of the model compared to the traditional least square regression model.  
72 The GWR model also improves the reliability of the relationship by reducing the  
73 spatial autocorrelation (Tu and Xia 2008). Economic development was the main  
74 factor in the changes in industrial wastewater discharge in each province during the  
75 study period (Geng et al. 2014). The spatial and temporal distribution characteristics  
76 of total wastewater discharge in 31 provinces in China from 2002 to 2013 were

77 analyzed (Chen et al. 2016). According to the results of spatial correlation analysis,  
78 the province's nitrogen oxide emissions changes not only affect the province itself, but  
79 also the neighboring areas (Diao et al.). A data set composed of 173 countries was  
80 used to estimate the EKC that was increased by neighboring per capita income and  
81 energy intensity (Zhang et al. 2019). The spatial correlation analysis using global and  
82 local Moran I value shown that a significant and positive spatial autocorrelation in  
83 environmental, economic and energy aspects, and cities in China was showing a trend  
84 of decoupling from economic development (Ma et al. 2020). The study found that  
85 encouraging cooperation between neighboring provinces may help reduce the IWD  
86 (Zhang et al. 2020). Economic development, investment in environmental  
87 governance, industrial structure, and technological innovation all had a certain impact  
88 on the amount of IWD, and also shown significant spatial spillover effects (Bu et al.  
89 2021).

90 In the current research on environmental pollution and economic development,  
91 some do not consider spatial factors, but do simple statistical analysis to study the  
92 linear relationship between environmental pollution and economic development. The  
93 environmental pollution in the early stage increases with economic growth, reaching a  
94 certain level. After that, it will decrease with the growth of the economic level,  
95 showing an inverted U-shape. Others only consider spatial factors, and had not  
96 studied the specific impact of spatial changes on environmental pollution data. This  
97 study will use panel data from 79 cities in the Yellow River Basin. In spatial analysis,  
98 by calculating different spatial matrices, the spatial influence was calculated

99 according to the Moran index. Then, in the Bayesian setting, Markov chain Monte  
100 Carlo simulation was used to include the spatial influence in the random effects, so  
101 that the error of the model was reduced, and the most suitable model for the discharge  
102 of industrial wastewater in the Yellow River Basin was found.

103

104     **2 Methods and data**

105     *2.1 Study area*

106       The Yellow River Basin refers to the geographic and ecological area affected by  
107       the river from the source to the sea. The relevant area of the Yellow River flowing  
108       through the provinces is often referred to as the Yellow River Basin. The Yellow River  
109       Basin has a very important position in my country's economic and social development  
110       and ecological security. The ecological protection and high-quality development of  
111       the Yellow River Basin are of great significance. According to the Yellow River  
112       Conservancy Commission's survey of the cities included in the Yellow River Basin, in  
113       figure 1, all city in Qinghai Province, Gansu Province, Ningxia Hui Autonomous  
114       Region, Inner Mongolia Autonomous Region, Sichuan Province, Shaanxi Province,  
115       Shanxi Province, Henan Province, and Shandong Province can be found. According to  
116       the availability of data and the convenience of research, 79 cities were selected for  
117       EKC analysis of their IWD and GRP.

118     *2.2 Data*

119       The data comes from the *China City Statistical Yearbook* in the National Bureau  
120       of Statistics (<http://www.stats.gov.cn/>), using data from various cities from 2003 to  
121       2019. Discharge of industrial wastewater refers to the total amount of waste water  
122       discharged outside the enterprise through all the outlets of the factory area of an  
123       industrial enterprise. In some enterprises, the mixed discharge of indirect cooling  
124       water and direct cooling water is inseparable and can be included in the statistics. The  
125       GRP refers to the final result of production activities of all permanent resident units in

126 a region in a certain period of time calculated at market prices. Therefore, the average  
127 value of each city's data from 2003 to 2019 is used, and logarithmic conversion of the  
128 volume of industrial waste water discharged (10000 tons) and gross regional product  
129 (10000 yuan).

130 *2.3 Model setting*

131 The EKC has different manifestations in different places. It is generally divided  
132 into a linear function curve. Environmental pollution has been increasing with the  
133 development of the economic level (1). It is also an inverted U-shaped curve. When  
134 the economic level reaches a certain level, people pay more attention to  
135 environmental pollution and begin to invest in environmental governance (2). The  
136 problem of environmental pollution began to decrease. Another is that the pollution  
137 problem first increases, after reaching a certain level, there is a certain decrease, and  
138 then it starts to increase (3).

139 
$$Y_k = \beta_0 + \beta_1 X_k + \varepsilon \quad (1)$$

140 
$$Y_k = \beta_0 + \beta_1 X_k + \beta_2 X_k^2 + \varepsilon \quad (2)$$

141 
$$Y_k = \beta_0 + \beta_1 X_k + \beta_2 X_k^2 + \beta_3 X_k^3 + \varepsilon \quad (3)$$

142 where,  $Y_k$  is logarithm of the IWD,  $X_k$  is logarithm of the GRP,  $\varepsilon \sim (0, \sigma^2)$ .

143 Many problems in spatial data analysis can be explained as image restoration  
144 problems. In archaeology and epidemiology, pixel-based Bayesian image analysis is  
145 reviewed. The problem of spatial data analysis can be solved by Bayesian method, in  
146 which the prior distribution includes known spatial relations (Besag et al. 1991). A  
147 new model of spatial dependence, including separate parameters for over-dispersion

148 and spatial dependence intensity. The new dependency structure is incorporated into a  
149 general linear mixed model to estimate disease incidence in small geographic areas.  
150 The hybrid model allows the local smoothing rate to be adjusted by estimating  
151 spatially correlated random effects. Computer simulation studies compare the new  
152 model with the built-in autoregressive model, independent model, and non-random  
153 effects model (Leroux et al. 2000). Taking the space factor into account, the error of  
154 the model is smaller. Spatial autocorrelation is usually used to represent data related to  
155 a set of non-overlapping regions. These data appear in a variety of applications such  
156 as agriculture, education, epidemiology, and image analysis. Spatial conditional  
157 autoregressive models are usually in a hierarchical Bayesian framework, based on  
158 MCMC simulation for reasoning. The CARBayes package in R language describes its  
159 implementation through MCMC simulation technology, and introduces the use of this  
160 model in two working examples in the field of housing price analysis and disease  
161 mapping. Disease mapping is the field of epidemiology, which estimates the spatial  
162 pattern of disease risk in an extended geographic area in order to identify areas with  
163 higher risk levels (Lee 2013). The Bayesian hierarchical model uses a combination of  
164 available co-occurrence data and a set of spatial random effects to represent the risk  
165 surface. These random effects include those used to simulate any excessive dispersion  
166 or spatial correlation in disease data. This is illustrated by using Bayesian analysis to  
167 apply conditional autoregressive models to phosphate data sets from archaeological  
168 areas. Conditional autoregressive models have been widely used to analyze spatial  
169 data in different fields such as population, economy, epidemiology, and geography, as

170 a model of potential and observed variables (De Oliveira 2012).

171  $Y_k | \mu_k \sim f(y_k | \mu_k, v^2)$  (4)

172  $E(Y_k) = \mu_k$ ,  $K$  is 79, 79 cities in study area,  $v^2 \sim (1, 0.01)$  inverse gamma prior  
173 distribution

174  $g(\mu_k) = X_k^T \beta + O_k + \psi_k$  (5)

175  $Y_k \sim N(\mu_k, v^2)$  (6)

176  $\psi_k | \psi_{-k}, W, \tau^2, \rho \sim N\left(\frac{\rho \sum_{i=1}^K w_{ki} \psi_i}{\rho \sum_{i=1}^K w_{ki} + 1 - \rho}, \frac{\tau^2}{\rho \sum_{i=1}^K w_{ki} + 1 - \rho}\right)$  (7)

177 In the Bayesian hierarchical function, the connection function is  $g(\mu_k)$ , the  
178 covariate matrix  $X = (X_1, \dots, X_k)$ , the offset  $O_k = (O_1, \dots, O_k)$ , the spatial structure  
179  $\psi_k = (\psi_1, \dots, \psi_k)$ , a multivariate Gaussian prior is assumed for regression parameter  $\beta$ ,  
180 where  $\beta \sim N(\mu_\beta \Sigma_\beta)$ ,  $\mu_\beta$  is the mean of  $\beta$ , diagonal variance matrix  $\Sigma_\beta$ ,  $\tau^2 \sim (1, 0.01)$   
181 inverse gamma distribution,  $\rho \sim (0, 1)$  uniform distribution,  $W$  is the spatial weight  
182 matrix.

183

184     **3 Results and Discussions**

185     *3.1 Data analysis*

186         According to the data of the statistical yearbook, it can be found from the  
187         analysis that of the 79 cities studied, Weifang had the highest industrial wastewater  
188         emissions, with 2,091 tons, the lowest was Qingshui City, at 246 tons, and the  
189         average industrial wastewater emissions across the Yellow River basin was 5,133  
190         tons. In the analysis of the GRP, the GRP of Guyuan City was the least, 1,411,914  
191         yuan, Qingdao was the largest, at 6 3,912,288 yuan, and the average GRP was  
192         13,429,594 yuan. There is a relationship between the GRP and the IWD, and also  
193         some spatial differences observe in the EKC. Qingdao City's regional gross domestic  
194         product is the largest, industrial wastewater emissions are not Weifang City, the city  
195         has begun to pay attention to environmental pollution, take certain measures to reduce  
196         pollutant emissions. Weifang City's industrial wastewater emissions, causing a lot of  
197         pollution to the environment, at the cost of environmental damage, but did not achieve  
198         a certain degree of economic development.

199     *3.2 Model selecting*

200         By comparing the mean square error (MSE) and root mean square error (RMSE)  
201         of the above models, the analysis found that the overall EKC in this study area is not  
202         much different, and the error of the model is relatively small in table 1. The  
203         calculation result is  $Y_k=593.94-113.36X_k+7.23X_k^2-0.15\beta_2X_k^3+\epsilon$ , in the figure 4a. In  
204         these cities in the Yellow River Basin, as the GRP increases, the discharge of  
205         industrial wastewater is still rising, and it is not downward trend.

206  $MSE = \frac{1}{n} \sum_{i=1}^n |\hat{y}_i - y_i|$  (8)

207  $RMSE = \sqrt{\frac{1}{n} \sum_{i=1}^n (\hat{y}_i - y_i)^2}$  (9)

208 In the Bayesian environment, using MCMC for inference, without calculating the  
 209 spatial weight, the parameter posterior distribution of  $X_k$ ,  $X_k^2$ ,  $X_k^3$  is shown in the  
 210 following table 2. The result of the model is  $Y_k = 491.51 - 94.11X_k + 6.03X_k^2 - 0.15\beta_2 X_k^3$ ,  
 211 in the figure 4b.

212 *3.3 Spatial analysis*

213 In general, observations from regional units that are close together tend to have  
 214 similar values. In the spatial analysis, the Moran index (Bivand et al. 2018) of the  
 215 IWD and the GRP was calculated separately, and it was found that there was a certain  
 216 degree of spatial autocorrelation, so the parameters of the model cannot be simply  
 217 determined, and the spatial factors must be considered. As shown in table 3, where z-  
 218 score is greater than 2.58, or p-value is less than 0.01, it can be explained that it is not  
 219 spatial randomness, but has a certain spatial correlation. And the spatial distribution  
 220 characteristics of IWD, the GRP and residuals ( $\varepsilon$ ) are obvious from fig 2a,2b,2c.

221  $I = \frac{\sum_{i=1}^n \sum_{j=1}^n W_{i,j} (X_i - \bar{X})(X_j - \bar{X})}{(\sum_{i=1}^n \sum_{j=1}^n W_{i,j}) \sum_{i=1}^n (X_i - \bar{X})^2}$  (10)

222 where, n is 79cities,  $X_i$  and  $X_j$  represent IWD in area i and j,  $\bar{X}$  is the average of IWD  
 223 in 79 cities, and  $W_{i,j}$  is the spatial weight matrix.

224 By calculating the Moran index of the model's residual, it is found that the error  
 225 also has a certain spatial agglomeration, so the model needs further parameter  
 226 determination. The residual autocorrelation reduces the error by using a set of  
 227 spatially correlated random effects to increase the linear predictor variable as part of

228 the Bayesian hierarchical model. Spatial random effects are taken into account and are  
229 usually expressed in conditional autoregressive models. The model induces spatial  
230 autocorrelation through the adjacent structure of regional units. Part of this spatial  
231 autocorrelation can be modeled by including known covariate risk factors in the  
232 regression model, but after considering these covariate effects, the spatial structure is  
233 usually retained in the residuals, which reduces the error of the model.

234 Then Choosing different spatial weight matrices for spatial analysis, where B is  
235 the basic binary code, that is, the spatial weight matrix with adjacent is 1 and non-  
236 adjacent is 0. W is the row standardization of B, C is the matrix standardization of B,  
237 U is equal to C divided by the number of neighbors, "minmax", the weight is divided  
238 by the minimum value of the maximum number of rows and the maximum number of  
239 columns of the input weight (Kelejian and Prucha 2010). The models without  
240 considering the spatial factors are calculated separately, and the Deviance Information  
241 Criteria (DIC) is 160.15. Compared with other weight matrices for calculating the  
242 spatial influence, it can be found that the DIC is the largest, so the spatial influence of  
243 the model needs to be included. Then, 4 different spatial weights were selected, and  
244 found that when the U matrix is selected, the DIC is -15.31, and the model has the  
245 smallest error, so the spatial weight matrix is selected as U for the next calculation, as  
246 shown in table 4.

247 We can write the Bayesian deviance (Bakar 2012) as:  $D(\theta) = -2L(\theta | y)$ ,  $L(\theta | y)$  is  
248 the log-likelihood of the model.

249 Now the goodness of fit of a model is obtained as  $\bar{D} = E_{\theta | y}(D)$  and the model

250 complexity is written as: $p_D = E_{\theta|y}(D) - D \left[ E_{\theta|y}(\theta) \right]$   
 251  $DIC = E_{\theta|y}(D) + p_D = D \left[ E_{\theta|y}(\theta) \right] + 2p_D$  (11)  
 252 Watanabe-Akaike information criteria  
 253  $WAIC = \sum_{i=1}^n \log E_{\theta|y}[f(y_i | \theta)] + \sum_{i=1}^n V_{\theta|y}[\log p(y_i | \theta)]$  (12)  
 254 Log pseudo marginal likelihood  
 255  $LPML = \sum_{i=1}^n \log \left[ f(y_i | y_{(-i)}) \right]$  (13)  
 256 *3.4 Bayesian inference*  
 257 After taking the spatial autocorrelation into account, the Bayesian hierarchical  
 258 model is adopted, and three Markov chains are selected for calculation. The inference  
 259 of this model is based on three parallel Markov chains. Each chain has run 300,000  
 260 samples, and 100000 have been deleted as the burning period. The remaining 200,000  
 261 samples were diluted 100 times, resulting in 6,000 samples used to infer 3 Markov  
 262 chains. The 3 Markov chains is calculated, the posterior distribution of the parameters  
 263 is shown in the table 5, and the posterior median of the parameters are -91.25, 5.86,  
 264 and -0.12 respectively, as shown in figure 3. The sample diagram of the simulated  
 265 parameters is as follows, and the parameters are all convergent.  
 266 It can be known through analysis, under the Bayesian hierarchical structure, the  
 267 spatial error is calculated. After a large number of MCMC simulations, it can be found  
 268 that the amount of IWD will be reduced in the cities in the Yellow River Basin and the  
 269 current the comparison. With the development of the economy, there will be more  
 270 investment in reducing IWD, which will eventually be the curve shown in the figure  
 271 4c. The entire Yellow River Basin, as a whole, will have spatial differences in

272 pollutant emissions, but it will be no spatial differences in the curve of the entire  
273 model.

274

275     **4 Conclusions**

276     This paper studies the discharge of industrial wastewater in prefecture-level cities  
277     in the Yellow River Basin, and analyzes the relationship between the discharge of  
278     industrial wastewater and the GRP. Results showed that both the amount of IWD and  
279     the GRP have a certain spatial autocorrelation, and the error of fitting using the EKC  
280     also has a certain spatial autocorrelation. The city with the largest amount of IWD is  
281     Weifang City, Qingdao City has the largest GRP, and Jiayuguan City has the largest  
282     error in the model. In the Bayesian environment, the inference found that the medians  
283     of the posterior parameter distributions of  $X_k$ ,  $X_k^2$ , and  $X_k^3$  are -91.25, 5.86, -0.12.  
284     Bayesian inference suggested the model of  $Y_k = 474.79 - 91.25X_k + 5.86X_k^2 - 0.12\beta_2X_k^3$ ,  
285     and the DIC of the model is -15.31. The discharge of industrial wastewater was  
286     increased with the increasing of GRP, and not showed a certain downward trend. The  
287     Bayesian hierarchical structure showed that the spatial error is calculated within the  
288     error. After a large number of MCMC simulations, it can be found that the amount of  
289     IWD in the cities of the Yellow River Basin should be less than it is now. Results also  
290     suggested that the prior space-time effects should be also considered in the  
291     spatiotemporal autoregressive model.

292

293     **Acknowledgments**

294     This paper thanks the National Bureau of Statistics (<http://www.stats.gov.cn/>) and  
295     the package CARBayes (<https://cran.r-project.org/web/packages/CARBayes>) in the  
296     open-source software R language (<https://www.r-project.org/>).

297

298     **Declarations**

299       **Ethical approval** Not applicable.

300       **Consent to participate** Not applicable.

301       **Consent to publish** Not applicable.

302       **Funding** Not applicable.

303       **Competing interests** All authors declare no competing interests.

304       **Availability of data and materials** All data generated or analyzed in the current

305 study was included in this article.

306       **Author contribution** Libo Xia: methodology, software, data analysis, writing—

307 original draft. Zhiliang Wang: writing—review and editing. Shuang Du: writing and

308 editing. Decun Tian: writing and editing. Feng Chen: writing and editing. All authors

309 read and approved the final manuscript.

310

311     **References**

312 Bakar KS (2012) Bayesian analysis of daily maximum ozone levels

313 Besag J, York J, Mollié A (1991) A Bayesian image restoration with two applications

314       in spatial statistics Ann Inst Statist Math 43: 1–59. Find this Article online 43:1–20

315 Bivand RS, David · , Wong WS, Wong DWS (2018) Comparing implementations of

316 global and local indicators of spatial association. TEST 27:716–748.

317 <https://doi.org/10.1007/s11749-018-0599-x>

318 Bu Y, Wang E, Jiang Z (2021) Evaluating spatial characteristics and influential

319 factors of industrial wastewater discharge in China: A spatial econometric

320 approach. Ecol Indic 121:107219.

321 <https://doi.org/10.1016/J.ECOLIND.2020.107219>

322 Chen K, Liu X, Ding L, et al (2016) Spatial characteristics and driving factors of

323 provincial wastewater discharge in China. Int J Environ Res Public Health 13:.

- 324           <https://doi.org/10.3390/IJERPH13121221>
- 325       Cheng Z, Li L, Liu J (2017) Identifying the spatial effects and driving factors of urban  
326           PM2.5 pollution in China. *Ecol Indic* 82:61–75.  
327           <https://doi.org/10.1016/j.ecolind.2017.06.043>
- 328       De Oliveira V (2012) Bayesian analysis of conditional autoregressive models. *Ann  
329           Inst Stat Math* 64:107–133. <https://doi.org/10.1007/s10463-010-0298-1>
- 330       Diao B, Ding L, Su P, Cheng J The Spatial-Temporal Characteristics and Influential  
331           Factors of NO<sub>x</sub> Emissions in China: A Spatial Econometric Analysis.  
332           <https://doi.org/10.3390/ijerph15071405>
- 333       Dinda S (2004) Environmental Kuznets Curve hypothesis: A survey. *Ecol Econ  
334           49:431–455.* <https://doi.org/10.1016/j.ecolecon.2004.02.011>
- 335       Du G, Liu S, Lei N, Huang Y (2018) A test of environmental Kuznets curve for haze  
336           pollution in China: Evidence from the penal data of 27 capital cities. *J Clean  
337           Prod* 205:821–827. <https://doi.org/10.1016/j.jclepro.2018.08.330>
- 338       Geng Y, Wang M, Sarkis J, et al (2014) Spatial-temporal patterns and driving factors  
339           for industrial wastewater emission in China. *J Clean Prod* 76:116–124.  
340           <https://doi.org/10.1016/j.jclepro.2014.04.047>
- 341       Grossman GM, Krueger AB (1995) Economic Growth and the Environment\*. *Q J  
342           Econ* 110:353–377. <https://doi.org/10.2307/2118443>
- 343       Kelejian HH, Prucha IR (2010) Specification and estimation of spatial autoregressive  
344           models with autoregressive and heteroskedastic disturbances. *J Econom* 157:53–  
345           67. <https://doi.org/10.1016/J.JECONOM.2009.10.025>
- 346       Kijima M, Nishide K, Ohyama A (2010) Economic models for the environmental  
347           Kuznets curve: A survey. *J Econ Dyn Control* 34:1187–1201.  
348           <https://doi.org/10.1016/j.jedc.2010.03.010>
- 349       Lee D (2013) CARBayes: An R package for Bayesian spatial modeling with  
350           conditional autoregressive priors. *J Stat Softw* 55:1–24.  
351           <https://doi.org/10.18637/jss.v055.i13>
- 352       Leroux BG, Lei X, Breslow N (2000) Estimation of Disease Rates in Small Areas: A  
353           new Mixed Model for Spatial Dependence. 179–191.

- 354 https://doi.org/10.1007/978-1-4612-1284-3\_4
- 355 Li Z, Song Y, Zhou A, et al (2020) Study on the pollution emission efficiency of  
356 China's provincial regions: The perspective of Environmental Kuznets curve. J  
357 Clean Prod 263:121497. https://doi.org/10.1016/J.JCLEPRO.2020.121497
- 358 Lin B, Zhu J (2018) Changes in urban air quality during urbanization in China. J  
359 Clean Prod 188:312–321. https://doi.org/10.1016/J.JCLEPRO.2018.03.293
- 360 Ma B, Tian G, Kong L (2020) Spatial-temporal characteristics of China's industrial  
361 wastewater discharge at different scales. Environ Sci Pollut Res 27:8103–8118.  
362 https://doi.org/10.1007/s11356-019-07488-7
- 363 Managi S (2006) Pollution, natural resource and economic growth: An econometric  
364 analysis. Int J Glob Environ Issues 6:73–88.  
365 https://doi.org/10.1504/IJGENVI.2006.009401
- 366 Ridzuan S (2019) Inequality and the environmental Kuznets curve. J Clean Prod  
367 228:1472–1481. https://doi.org/10.1016/J.JCLEPRO.2019.04.284
- 368 Selden TM, Song D (1994) Environmental quality and development: Is there a  
369 kuznets curve for air pollution emissions? J. Environ. Econ. Manage. 27:147–  
370 162
- 371 Shahbaz M, Sinha A (2019) Environmental Kuznets curve for CO2 emissions: a  
372 literature survey. J Econ Stud 46:106–168. https://doi.org/10.1108/JES-09-2017-  
373 0249
- 374 Stern DI (2004) The Rise and Fall of the Environmental Kuznets Curve. World Dev  
375 32:1419–1439. https://doi.org/10.1016/j.worlddev.2004.03.004
- 376 Tu J, Xia ZG (2008) Examining spatially varying relationships between land use and  
377 water quality using geographically weighted regression I: Model design and  
378 evaluation. Sci Total Environ 407:358–378.  
379 https://doi.org/10.1016/j.scitotenv.2008.09.031
- 380 Ulucak R, Bilgili F (2018) A reinvestigation of EKC model by ecological footprint  
381 measurement for high, middle and low income countries. J Clean Prod 188:144–  
382 157. https://doi.org/10.1016/J.JCLEPRO.2018.03.191
- 383 Yao S, Zhang S, Zhang X (2019) Renewable energy, carbon emission and economic

384 growth: A revised environmental Kuznets Curve perspective. *J Clean Prod*  
385 235:1338–1352. <https://doi.org/10.1016/J.JCLEPRO.2019.07.069>

386 Zhang P, Yang D, Zhang Y, et al (2020) Re-examining the drive forces of China's  
387 industrial wastewater pollution based on GWR model at provincial level. *J Clean*  
388 *Prod* 262:121309. <https://doi.org/10.1016/j.jclepro.2020.121309>

389 Zhang WW, Sharp B, Xu SC (2019) Does economic growth and energy consumption  
390 drive environmental degradation in China's 31 provinces? New evidence from a  
391 spatial econometric perspective. *Appl Econ* 51:4658–4671.  
392 <https://doi.org/10.1080/00036846.2019.1593943>

393 Zhao X, Zhou W, Han L, Locke D (2019) Spatiotemporal variation in PM<sub>2.5</sub>  
394 concentrations and their relationship with socioeconomic factors in China's  
395 major cities. *Environ Int* 133:105145.  
396 <https://doi.org/10.1016/J.ENVINT.2019.105145>

397

398 **TABLES**

399 Table 1 Model comparison table

Model	MSE	RMSE	Adjusted R <sup>2</sup>
$Y_k = \beta_0 + \beta_1 X_k + \epsilon$	0.43	0.6559	0.5698
$Y_k = \beta_0 + \beta_1 X_k + \beta_2 X_k^2 + \epsilon$	0.427	0.6532	0.5734
$Y_k = \beta_0 + \beta_1 X_k + \beta_2 X_k^2 + \beta_3 X_k^3 + \epsilon$	0.414	0.6431	0.5864

400

401 Table 2 The parameter posterior distribution table has no spatial influence

	50%	2. 5%	97. 5%
Intercept	491. 51	-125. 75	1093. 62
$X_k$	-94. 11	-207. 07	22. 24
$X_k^2$	6. 03	-1. 19	13. 06
$X_k^3$	-0. 13	-0. 27	0. 02

402

403 Table 3 Moran Index Table

	IWD	GRP	$\varepsilon$
I	0.52	0.322754	0.17
z-score	9.220178	5.873645	3.16
p-value	0	0	0.0015

404

405 Table 4 Model selection with different spatial weights

Spatial matrix	weight	DIC	WAIC	LMPL
None		160. 15	161. 99	-81. 13
B		83. 82	137. 18	-70. 82
C		60. 24	134. 30	-70. 07
minmax		25. 89	127. 59	-60. 92
U		-15. 31	117. 03	-57. 31

406

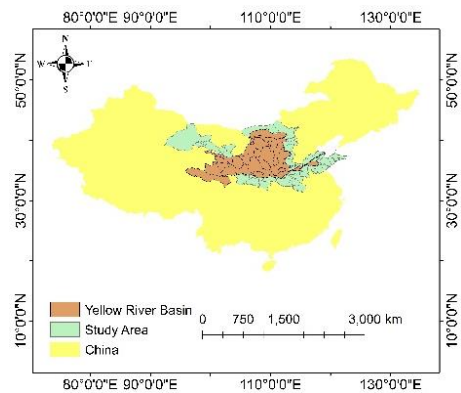
407 Table 5 Parameter posterior distribution table

	50%	2. 5%	97. 5%
Intercept	474. 79	-127. 81	1073. 32
X <sub>k</sub>	-91. 25	-203. 25	21. 15
X <sub>k</sub> <sup>2</sup>	5. 86	-1. 17	12. 81
X <sub>k</sub> <sup>3</sup>	-0. 12	-0. 26	0. 02

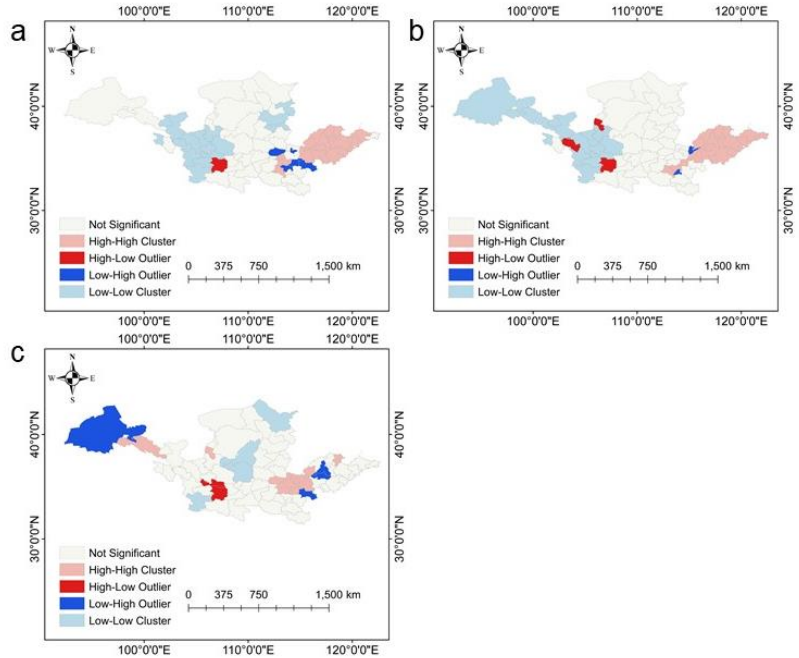
408

409 **FIGURES**

410



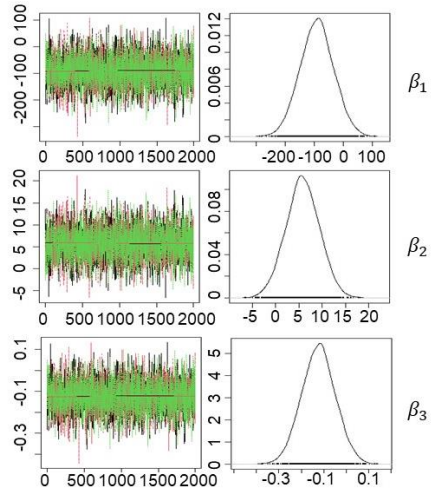
411 Fig 1 The map of the study area including 79 cities in the Yellow River Basin.



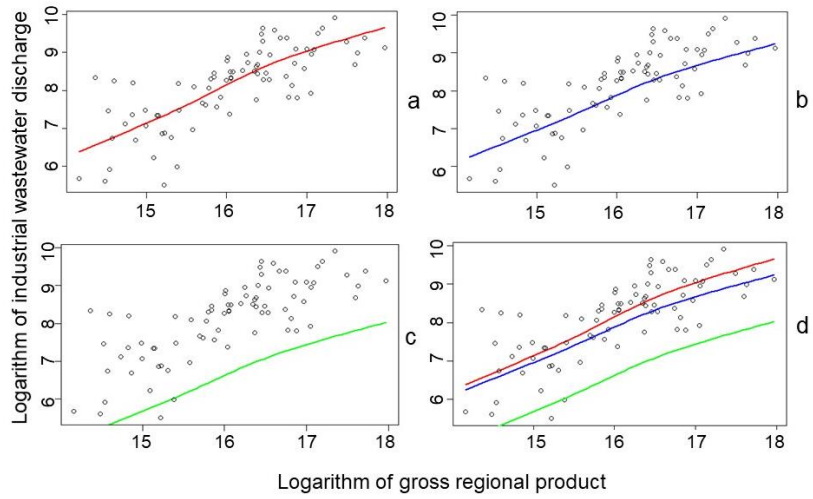
412

413 Fig 2 Spatial clustering of IWD, GRP and  $\epsilon$  in 79 cities.

414



415 Fig 3 Convergence graph of Markov chains with posterior distribution of parameters  $\beta_1, \beta_2, \beta_3$ .



416

417 Fig 4 The fitting graphs, a is simple EKC, b is the model of autoregressive priors in Bayesian  
 418 without spatial, and c is spatial autoregressive model in Bayesian setting, d is comparison among  
 419 a, b and c.